Supporting Information: **Calculation of dielectric spectra of a glucose-based deep eutectic solvent: Insights from classical molecular dynamics simulation**

Soham Sarkar*

Manufacturing Futures Lab, Department of Chemical Engineering,

University College London, London, E20 2AE, UK

Email: soham9038@gmail.com

1. System information

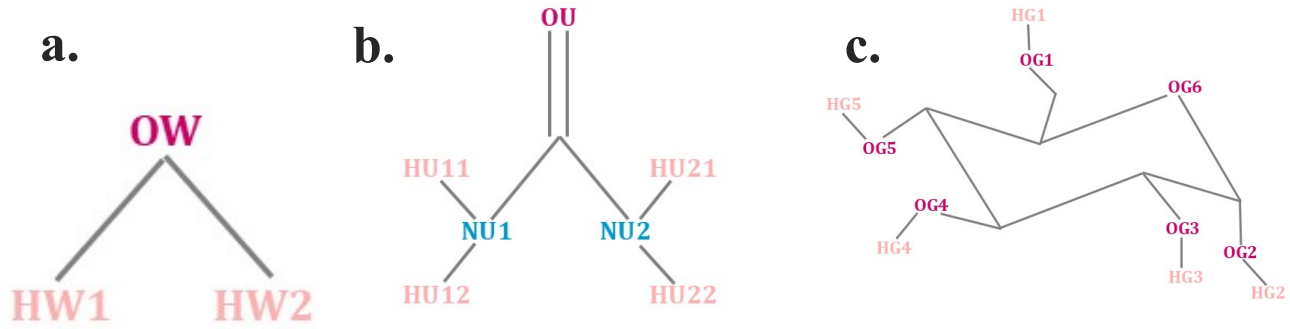

Figure S1: Schematic representation of the structure of **a.** water, **b.** urea, **c.** glucose. Relevant atom name, used in calculations, are mentioned.

System	# Water	# Urea	# Glucose	Temperature (K)	$\rho_{Simulation}$ (gm/cm^3)	$\rho_{Reference}$ (gm/cm^3)
BW	1000	--	--	298	0.99	0.99[1]
UW	1000	27	--	298	1.02	1.02[2]
GW	1000	--	27	300	1.08	1.07[3]

Table S1: System information and density calculations of the control simulations.

2. Calculation of dielectric spectra of test systems

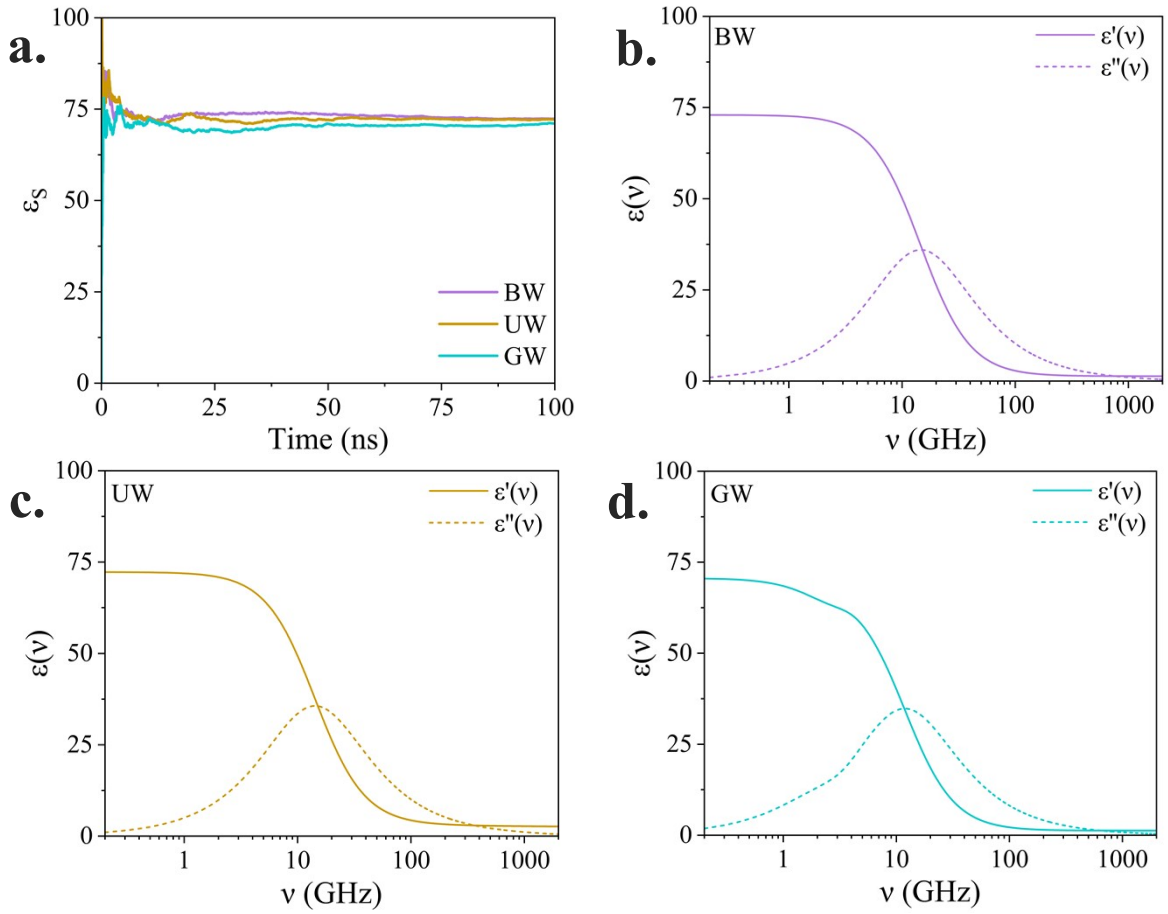

Figure S2: a. Time evolution of the static dielectric constant (ε_S) calculated for the BW, UW, and GW systems. Frequency dependent real (ε'_ν), and imaginary (ε''_ν) part of the dielectric spectra for **b.** BW, **c.** UW, and **d.** GW systems.

Classical simulation with fixed-charge force field underestimates the static dielectric constant of bulk water and aqueous solute solutions. Modeled ε_S values are 73 (BW), 72 (UW) and 71 (GW) versus experimental values of ~78[2], ~85[2] and ~75[4]. While simulation almost quantitatively reproduces ε_S for the GW system, it underestimates in case of BW and UW system. This behaviour can be attributed to the known limitations of non-polarizable force fields, which do not include electronic polarization and can underestimate molecular dipoles and solute-solvent correlations. On the other hand, the obtained dielectric loss peak between 10 to 20 GHz, are evident of the precise estimation of the dynamic behaviour of the control systems by the existing forcefield.[2,4]

3. Calculation of dielectric spectra of NADES system

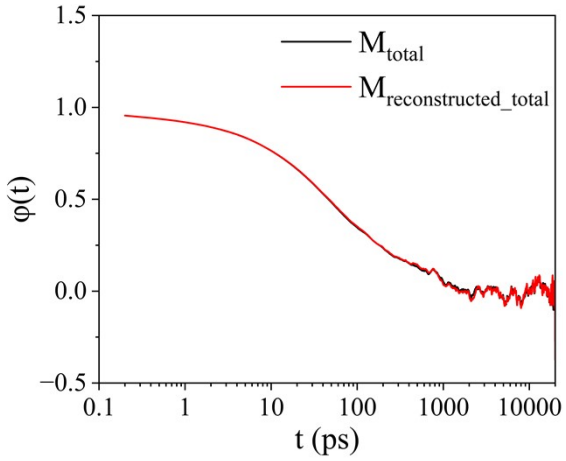

Figure S3: Validation of Equation 9 of the main manuscript.

To validate the decomposition of the total dipole moment M into self and cross components, we compute the normalized autocorrelation function using two independent approaches. For this validation, we follow Equation 9 of the main manuscript. In the first approach, the normalized autocorrelation function is calculated directly from the total dipole moment M of the system, corresponding to the left-hand side of Equation 9. This result is shown in Figure S3 as the black curve, labelled M_{total}. In the second approach, we evaluated the normalized autocorrelation function by separately considering the self and cross components, as represented on the right-hand side of Equation 9. The resulting curve is shown in Figure S3 in red and labelled $M_{reconstructed\_total}$. As evident from Figure S3, the two curves exhibit excellent agreement, confirming the validity and applicability of Equation 9 for our system.

	a_1	τ_1 (ps)	a_2	τ_2 (ps)	a_3	τ_3 (ps)	a_4	τ_4 (ps)	a_5	τ_5 (ps)
Single	--	--	--	--	--	--	--	--	1	134.59
Bi	--	--	--	--	0.62	32.05	--	--	0.38	476.23
Tri	--	--	0.13	2.06	0.51	42.81	--	--	0.36	490.87
Tetra	--	--	0.13	2.06	0.42	42.81	0.09	42.81	0.36	490.83
Penta	0.06	0.19	0.08	4.82	0.34	43.64	0.17	43.63	0.35	491.45

Table S2: Timescale and corresponding contributions obtained from mono to penta-fitted normalized autocorrelation function related to the relaxation of the total dipole moment (M) of the system.

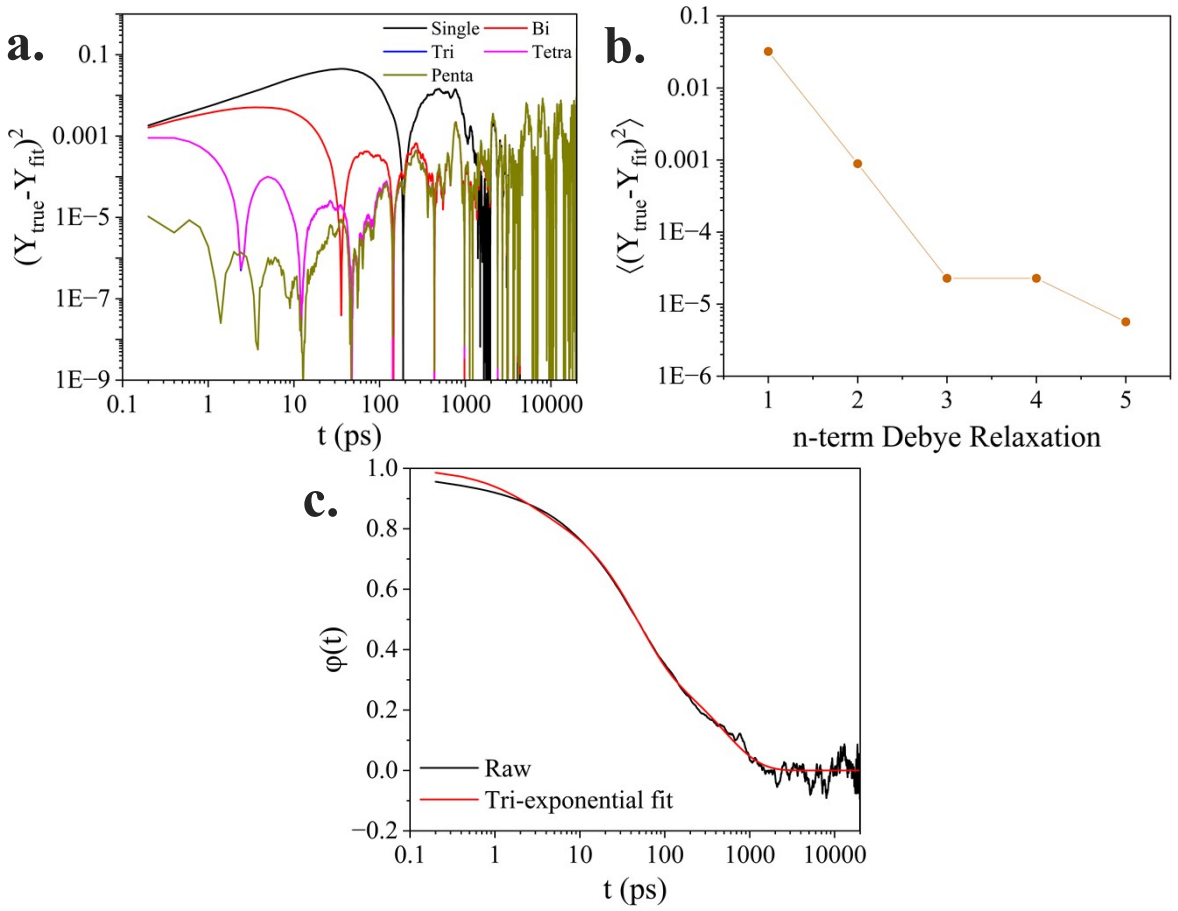

Figure S4: a. Lag-time dependence of the deviation of fitted data from the raw normalized autocorrelation data, **b.** n-term exponential decay dependence of the average deviation of fitted data from the raw normalized autocorrelation data. 'n' varies from 1 to 5, **c.** Comparison of raw and tri-exponentially fitted normalized autocorrelation data.

Table S2 presents the fitting results of the raw dynamical data using an n-term Debye relaxation function, where n varies from 1 to 5. To determine the optimal value of n, we employ a deviation metric defined as $(Y_{true} - Y_{fit})^2$, where Y_{true} and Y_{fit} represent the simulation-generated and fitted values, respectively. As shown in Figure S4.a., the differences among the various *n*-term fits are most pronounced at short times, while beyond 1 ns, the curves nearly overlap. Figure S4.b. shows the average deviation, computed over all lag time points, plotted as a function of *n*. The resulting elbow-type curve clearly indicates that *n* = 3 provides the optimal fitting condition, yielding an average deviation in the order of 10^{-5}. Figure S4.c. displays the raw normalized autocorrelation data along with the tri-exponential fit, demonstrating excellent agreement between the two.

	a_1	τ_1 (ps)	a_2	τ_2 (ps)	a_3	τ_3 (ps)
Glucose						
Single	--	--	--	--	1	246.11
Bi	--	--	0.52	45.89	0.48	581.43
Tri	0.14	1.99	0.41	69.37	0.45	603.65
Urea						
Single	--	--	1	52.06	--	--
Bi	--	--	0.67	24.23	0.33	149.48

Tri	0.24	5.48	0.67	55.12	0.09	356.94
Water						
Single	--	--	1	37.53	--	--
Bi	--	--	0.84	21.32	0.16	349.43
Tri	0.29	3.13	0.60	38.73	0.11	485.09
Urea-Water						
Single	--	--	1	97.19	--	--
Bi	--	--	0.67	28.48	0.33	417.59
Tri	0.20	28.47	0.47	28.47	0.33	471.54
Water-Glucose						
Single	--	--	--	--	1	235.49
Bi	--	--	0.47	42.27	0.53	478.73
Tri	0.03	0.97	0.45	45.07	0.52	480.19
Glucose-Urea						
Single	--	--	--	--	1	334.41
Bi	--	--	0.31	16.58	0.69	475.81
Tri	0.11	16.54	0.20	16.61	0.69	475.76

Table S3: Timescale and corresponding contributions obtained from the single-, bi-, tri-exponentially fitted normalized autocorrelation function related to the total dipole relaxation of all possible self and cross combinations of the components.

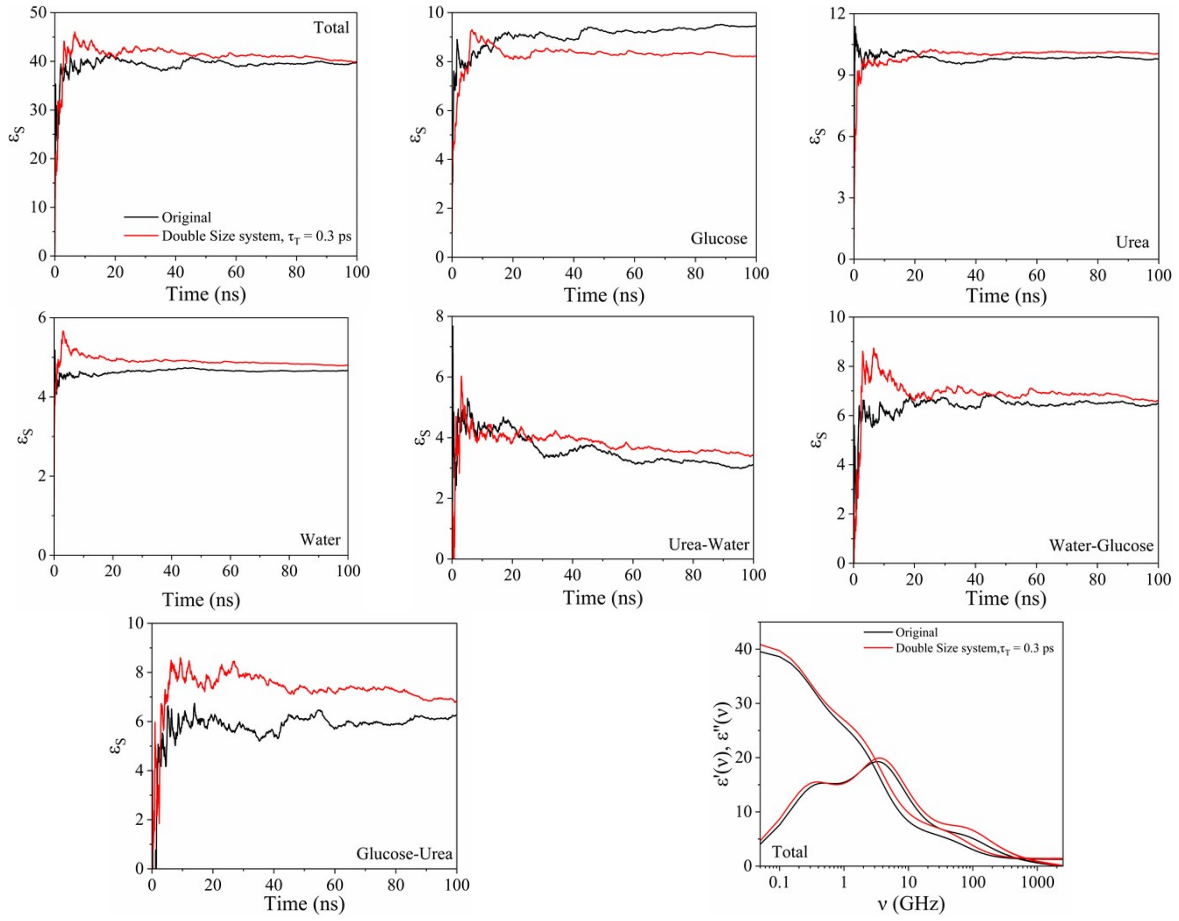

Figure S5: Comparison of dielectric properties between original system (black), and newly constructed large system with $\tau_T =$ 0.3 ps (red) respectively.

RDF combination	r_c (nm)
Water	
OW-OW	0.35
Urea	
NU-OU	0.43
NU-NU	0.45
Glucose	
OG1-OG1	0.35
OG1-OG2	0.38
OG1-OG3	0.36
OG1-OG4	0.38
OG1-OG5	0.36
OG1-OG6	0.40
OG2-OG2	0.40
OG2-OG3	0.37
OG2-OG4	0.36
OG2-OG5	0.39
OG2-OG6	0.40
OG3-OG3	0.39
OG3-OG4	0.35
OG3-OG5	0.38
OG3-OG6	0.40
OG4-OG4	0.38
OG4-OG5	0.35
OG4-OG6	0.40
OG5-OG5	0.35
OG5-OG6	0.40
Urea-Water	
NU-OW	0.45
OU-OW	0.43
Water-Glucose	
OW-OG1	0.35
OW-OG2	0.40
OW-OG3	0.38
OW-OG4	0.37
OW-OG5	0.35
OW-OG6	0.35

Glucose-Urea	
OG1-OU	0.35
OG2-OU	0.40
OG3-OU	0.40
OG4-OU	0.35
OG5-OU	0.35
OG1-NU	0.41
OG2-NU	0.42
OG3-NU	0.41
OG4-NU	0.40
OG5-NU	0.41
OG6-NU	0.38

Table S4: Position of first minima (r_c) obtained from the g(r) plot of different combinations of donor-acceptor atoms.

Combinations	Hydrogen bond relaxation time (ps)			
	Bi exponential		Tri exponential	
	a_i	τ_i	a_i	τ_i
$\langle\tau_{HU\rightarrow OW}\rangle$	0.70 (±0.00)	0.48 (±0.00)	0.59 (±0.00)	0.21 (±0.00)
			0.34 (±0.00)	15.40 (±0.13)
	0.30 (±0.00)	36.18 (±0.49)	0.07 (±0.00)	171.69 (±1.03)
$\langle\tau_{HW\rightarrow OU}\rangle$	0.79 (±0.00)	1.07 (±0.01)	0.58 (±0.00)	0.27 (±0.00)
			0.35 (±0.00)	9.49 (±0.03)
	0.21 (±0.00)	46.77 (±0.28)	0.07 (±0.00)	152.75 (±1.01)
$\langle\tau_{HW\rightarrow NU}\rangle$	0.87 (±0.00)	0.15 (±0.00)	0.79 (±0.0002)	0.10 (±0.00)
			0.18 (±0.0002)	6.54 (±0.01)
	0.13 (±0.00)	21.55 (±0.12)	0.03 (±0.0000)	140.76 (±0.49)

Table S5: Timescale and corresponding contributions obtained from the bi-, and tri-exponentially fitted normalized autocorrelation function related to the hydrogen bond relaxation between atoms of urea and water molecules. We provide the std. dev. of the calculation in the bracket.

Combinations	Hydrogen bond relaxation time (ps)			
	Bi exponential		Tri exponential	
	a_i	τ_i	a_i	τ_i
$\langle\tau_{HG1\rightarrow OW}\rangle$	0.64 (±0.00)	2.38 (±0.06)	0.44 (±0.00)	0.42 (±0.01)

			0.42 (±0.00)	21.31 (±0.59)
	0.36 (±0.00)	70.22 (±1.33)	0.14 (±0.00)	155.02 (±2.94)
$\langle\tau_{HG2\rightarrow OW}\rangle$	0.59 (±0.00)	3.89 (±0.09)	0.38 (±0.00)	0.48 (±0.02)
			0.43 (±0.01)	28.52 (±0.59)
	0.41 (±0.00)	96.05 (±1.15)	0.19 (±0.01)	175.89 (±3.64)
$\langle\tau_{HG3\rightarrow OW}\rangle$	0.62 (±0.00)	3.54 (±0.08)	0.40 (±0.00)	0.49 (±0.01)
			0.46 (±0.00)	25.79 (±0.81)
	0.38 (±0.00)	80.94 (±0.89)	0.14 (±0.00)	185.43 (±6.47)
$\langle\tau_{HG4\rightarrow OW}\rangle$	0.62 (±0.01)	7.82 (±0.15)	0.35 (±0.00)	1.24 (±0.04)
			0.49 (±0.00)	36.67 (±0.62)
	0.38 (±0.01)	120.74 (±2.81)	0.16 (±0.00)	238.46 (±4.91)
$\langle\tau_{HG5\rightarrow OW}\rangle$	0.56 (±0.00)	4.62 (±0.04)	0.35 (±0.00)	0.73 (±0.01)
			0.47 (±0.00)	30.88 (±0.42)
	0.44 (±0.00)	86.66 (±0.56)	0.18 (±0.00)	177.55 (±2.91)
$\langle\tau_{HW\rightarrow OG1}\rangle$	0.75 (±0.00)	5.09 (±0.03)	0.40 (±0.00)	0.96 (±0.02)
			0.47 (±0.00)	18.08 (±0.17)
	0.25 (±0.00)	96.12 (±0.98)	0.13 (±0.00)	182.51 (±2.24)
$\langle\tau_{HW\rightarrow OG2}\rangle$	0.74 (±0.00)	0.89 (±0.01)	0.55 (±0.00)	0.20 (±0.00)
			0.34 (±0.00)	11.38 (±0.07)
	0.26 (±0.00)	51.14 (±0.50)	0.11 (±0.00)	126.40 (±1.27)
$\langle\tau_{HW\rightarrow OG3}\rangle$	0.74 (±0.00)	4.19 (±0.03)	0.41 (±0.00)	0.65 (±0.01)
			0.47 (±0.00)	16.11 (±0.13)
	0.26 (±0.03)	83.54 (±0.73)	0.12 (±0.00)	164.03 (±1.63)
$\langle\tau_{HW\rightarrow OG4}\rangle$	0.74 (±0.00)	3.95 (±0.03)	0.42 (±0.00)	0.70 (±0.01)
			0.47 (±0.00)	15.92 (±0.17)
	0.26 (±0.00)	76.34 (±0.42)	0.11 (±0.00)	165.41 (±1.59)
$\langle\tau_{HW\rightarrow OG5}\rangle$	0.73 (±0.01)	4.41 (±0.03)	0.40 (±0.00)	0.77 (±0.01)
			0.46 (±0.00)	16.19 (±0.18)
	0.27 (±0.01)	83.87 (±0.94)	0.14 (±0.00)	151.78 (±2.22)
$\langle\tau_{HW\rightarrow OG6}\rangle$	0.71 (±0.00)	2.09 (±0.02)	0.46 (±0.00)	0.28 (±0.00)
			0.40 (±0.00)	14.00 (±0.18)
	0.29 (±0. 00)	68.53 (±0.80)	0.14 (±0.00)	136.44 (±2.38)

Table S6: Timescale and corresponding contributions obtained from the bi-, and tri-exponentially fitted normalized autocorrelation function related to the hydrogen bond relaxation between atoms of water and glucose molecules. We provide the std. dev. of the calculation in the bracket.

Combinations	Hydrogen bond relaxation time (ps)			
	Bi exponential		Tri exponential	
	a_i	τ_i	a_i	τ_i
$\langle\tau_{HG1\rightarrow OU}\rangle$	0.73 (±0.00)	0.88 (±0.02)	0.61 (±0.00)	0.23 (±0.00)
			0.31 (±0.00)	40.42 (±0.79)
	0.27 (±0.00)	123.49 (±2.27)	0.08 (±0.00)	430.18 (±18.61)
$\langle\tau_{HG2\rightarrow OU}\rangle$	0.66 (±0.00)	0.95 (±0.02)	0.56 (±0.00)	0.26 (±0.00)
			0.36 (±0.00)	41.23 (±0.79)
	0.34 (±0.00)	99.37 (±1.58)	0.08 (±0.00)	369.62 (±9.26)
$\langle\tau_{HG3\rightarrow OU}\rangle$	0.68 (±0.00)	1.46 (±0.03)	0.54 (±0.00)	0.27 (±0.00)
			0.36 (±0.00)	32.25 (±0.58)
	0.32 (±0.00)	112.81 (±1.53)	0.10 (±0.00)	351.88 (±6.37)
$\langle\tau_{HG4\rightarrow OU}\rangle$	0.66 (±0.00)	2.04 (±0.05)	0.51 (±0.00)	0.38 (±0.00)
			0.39 (±0.00)	37.85 (±0.56)
	0.34 (±0. 00)	107.54 (±2.93)	0.10 (±0.00)	353.12 (±9.32)
$\langle\tau_{HG5\rightarrow OU}\rangle$	0.67 (±0.00)	1.29 (±0.03)	0.54 (±0.00)	0.26 (±0.00)
			0.36 (±0.00)	33.26 (±0.44)
	0.33 (±0.00)	95.56 (±1.78)	0.10 (±0.00)	293.39 (±9.13)
$\langle\tau_{HG1\rightarrow NU}\rangle$	0.82 (±0.00)	0.19 (±0.00)	0.75 (±0.00)	0.13 (±0.00)
			0.20 (±0.00)	27.36 (±0.29)
	0.18 (±0.00)	77.73 (±0.63)	0.05 (±0.00)	328.51 (±6.49)
$\langle\tau_{HG2\rightarrow NU}\rangle$	0.80 (±0.00)	0.17 (±0.00)	0.74 (±0.00)	0.12 (±0.00)
			0.21 (±0.00)	25.76 (±0.22)
	0.20 (±0.00)	63.38 (±0.41)	0.05 (±0.00)	256.36 (±3.66)
$\langle\tau_{HG3\rightarrow NU}\rangle$	0.80 (±0.00)	0.20 (±0.00)	0.73 (±0.00)	0.12 (±0.00)
			0.22 (±0.00)	23.58 (±0.21)
	0.20 (±0.00)	64.62 (±0.80)	0.05 (±0.00)	257.16 (±3.76)
$\langle\tau_{HG4\rightarrow NU}\rangle$	0.80 (±0.00)	0.19 (±0.00)	0.73 (±0.00)	0.13 (±0.00)
			0.21 (±0.00)	20.81 (±0.32)
	0.20 (±0.00)	55.56 (±0.41)	0.05 (±0.00)	210.98 (±4.49)
$\langle\tau_{HG5\rightarrow NU}\rangle$	0.79 (±0.00)	0.20 (±0.00)	0.72 (±0.00)	0.13 (±0.00)
			0.22 (±0.00)	24.67 (±0.22)
	0.21 (±0.00)	68.06 (±0.92)	0.06 (±0.00)	231.37 (±3.11)
$\langle\tau_{HU\rightarrow OG1}\rangle$	0.67 (±0.00)	0.79 (±0.01)	0.57 (±0.00)	0.28 (±0.00)
			0.37 (±0.00)	30.72 (±0.20)

	0.33 (±0.00)	65.39 (±0.87)	0.06 (±0.00)	361.49 (±4.26)
$\langle\tau_{HU\rightarrow OG2}\rangle$	0.70 (±0.00)	0.59 (±0.01)	0.60 (±0.00)	0.21 (±0.00)
			0.33 (±0.00)	34.25 (±0.35)
	0.30 (±0.02)	82.57 (±1.82)	0.07 (±0.00)	355.15 (±4.75)
$\langle\tau_{HU\rightarrow OG3}\rangle$	0.66 (±0.00)	0.75 (±0.02)	0.56 (±0.00)	0.27 (±0.00)
			0.37 (±0.00)	32.08 (±0.20)
	0.34 (±0.00)	68.74 (±0.76)	0.07 (±0.00)	334.02 (±4.39)
$\langle\tau_{HU\rightarrow OG4}\rangle$	0.65 (±0.00)	0.80 (±0.03)	0.55 (±0.00)	0.27 (±0.00)
			0.38 (±0.00)	30.27 (±0.20)
	0.35 (±0.00)	65.98 (±0.64)	0.07 (±0.00)	291.90 (±4.67)
$\langle\tau_{HU\rightarrow OG5}\rangle$	0.66 (±0.00)	0.87 (±0.02)	0.55 (±0.00)	0.27 (±0.00)
			0.38 (±0.00)	32.10 (±0.23)
	0.34 (±0.00)	71.12 (±0.67)	0.07 (±0.00)	323.06 (±4.19)
$\langle\tau_{HU\rightarrow OG6}\rangle$	0.65 (±0.00)	0.96 (±0.01)	0.53 (±0.00)	0.24 (±0.00)
			0.37 (±0.00)	35.34 (±0.38)
	0.35 (±0.00)	89.25 (±1.61)	0.10 (±0.00)	280.60 (±4.07)

Table S7: Timescale and corresponding contributions obtained from the bi-, and tri-exponentially fitted normalized autocorrelation function related to the hydrogen bond relaxation between atoms of glucose and urea molecules. We provide the std. dev. of the calculation in the bracket.

References

1 The Engineering ToolBox (2003). Water Density, Specific Weight and Thermal Expansion Coefficients - Temperature and Pressure Dependence., https://www.engineeringtoolbox.com/water-density-specific-weight-d_595.html, (accessed October 13, 2025).

2 Y. Hayashi, Y. Katsumoto, S. Omori, N. Kishii and A. Yasuda, Liquid Structure of the Urea−Water System Studied by Dielectric Spectroscopy, *J. Phys. Chem. B*, 2007, **111**, 1076–1080.

3 M. Hossain, N. Chowdhury, A. Atahar and M. A. B. Hasan Susan, Water structure modification by d -(+)-glucose at different concentrations and temperatures-effect of mutarotation, *RSC Advances*, 2023, **13**, 19195–19206.

4 K. Shiraga, T. Suzuki, N. Kondo, T. Tajima, M. Nakamura, H. Togo, A. Hirata, K. Ajito and Y. Ogawa, Broadband dielectric spectroscopy of glucose aqueous solution: Analysis of the hydration state and the hydrogen bond network, *J. Chem. Phys.*, 2015, **142**, 234504.